J. Electrochem. Sci. Eng. **16** (2026) 3168; https://doi.org/10.5599/jese.3168

Open Access : : ISSN 1847-9286
https://pub.iapchem.org/ojs/index.php/JESE

Original scientific paper

Validation of a low-cost carbon screen-printed electrode platform: a statistical approach

Juliene Morais de Faria[1], Thomaz Henrique da Cunha Reis[2], Larissa Silva de Azevedo[3], Caio Henrique Pinke Rodrigues[1], Aline Thaís Bruni[1] and Marcelo Firmino de Oliveira[1,✉]

[1]*Departamento de Química. Faculdade de Filosofia, Ciências e Letras de Ribeirão Preto. Universidade de São Paulo (DQ/FFCLRP/USP), Avenida Bandeirantes, 3900, Bairro Monte Alegre, Ribeirão Preto - SP, CEP 14040-901, Brazil*
[2]*Faculdade de Direito de Ribeirão Preto - Universidade de São Paulo (FDRP/USP), Avenida Bandeirantes, 3900, Bairro Monte Alegre, Ribeirão Preto - SP, CEP 14040-901, Brazil*
[3]*Instituto de Química de São Carlos, Universidade de São Paulo (IQSC/USP), Avenida Trabalhador São Carlense, 400, Parque Arnold Schimidt, São Carlos - SP, CEP 14040-901, Brazil*

Corresponding Author: E-mail: ✉*marcelex@usp.br*

Received: December 15, 2025; Accepted: April 3, 2025; Published: April 10, 2026

Abstract

Electrochemical sensors have gained increasing attention for their high selectivity and sensitivity. Screen-printed electrodes (SPEs) are particularly attractive as low-cost, disposable, and scalable platforms that enable miniaturized electrochemical cells and field-deployable measurements. Here, we report a low-cost and easily fabricated carbon paste -SPE platform consisting of a 3D-printed acrylonitrile butadiene styrene body filled with carbon paste (graphite/mineral oil, 70:30) and a silver-ink pseudo-reference electrode. The device was evaluated using potassium ferricyanide (5.0 mmol L^{-1} in 0.5 mol L^{-1} KCl) as a redox probe. The i_{pa}/i_{pc} ratio was close to unity, while the peak-to-peak separation ($\Delta E_p \approx 949$ mV) indicated kinetic/ohmic contributions typical of composite carbon-based printed electrodes. A linear relationship between the corrected anodic peak current (i_{ap}) and the square root of the scan rate ($v^{1/2}$) yielded an electroactive area of 0.485 cm², substantially larger than the geometric area, consistent with surface heterogeneity/porosity. Statistical validation by ANOVA confirmed good repeatability and reproducibility ($p > 0.05$, 95 % confidence). Overall, the proposed CP-SPE provides a robust and reproducible low-cost platform with strong potential for voltammetric sensing applications.

Keywords

Electrochemical sensors; voltammetry; electrochemical validation; statistical techniques; repeatability; reproducibility

Introduction

Electrochemical sensors are a promising class of chemical sensors due to their high selectivity and sensitivity. They are particularly effective for determining the concentrations of various analytes in samples, including liquids and dissolved solids [1]. Compared to other sensor types, electrochemical sensors are attractive because of their high detectability, simplicity, and low cost [2-9]. The main categories of electrochemical sensors include potentiometric, amperometric, conductometric, and voltammetric devices.

In a voltammetric sensor, the redox reaction generates a current proportional to the concentration of the electroactive analyte [10]. Voltammetric methods are widely used to investigate electrode kinetics, elucidate redox mechanisms, determine thermodynamic constants, and quantify chemical species [11].

Voltammetric curves are obtained using a three-electrode system: a working electrode, which may be made of metallic or carbonaceous materials (*e.g*. platinum, gold, graphite, glassy carbon), an auxiliary electrode and a reference electrode [11,12]. Screen-printed electrodes (SPEs) are fabricated by printing inks onto polymeric or ceramic substrates [13]. Recently, SPEs have become increasingly important in electrochemical detection due to their affordability [14-16], scalability [17,18], and the ability to miniaturize the electrochemical cell [15,19]. This miniaturization reduces the required sample volume to a few microliters and decreases the overall size of the diagnostic system in which the device is integrated [20].

The development and use of new SPEs have expanded, with applications in diverse fields such as biosensing [20,21], environmental analysis [22], forensic science [23-26], and food [27] analysis [28]. An essential step in developing new SPEs is their validation [29]. This is commonly achieved through electroanalytical studies, in which quality parameters are determined using linear least-squares regression. This approach assumes a linear relationship between the measured quantity (*e.g.* concentration, volume, or activity (denoted as x_i) and the instrumental response (y_i), described by the equation $y_i = mx_i + b$ [11,30]. From the resulting regression curves and associated data, various parameters can be derived to assess the measurement system, including sensitivity, limit of detection, limit of quantification, repeatability, and reproducibility [11].

Beyond electrochemical characterization, statistical evaluation is a key step in electrochemical sensor development, particularly for low-cost platforms intended for routine or field use [31,32]. Recent literature has emphasized that many sensors fail to translate beyond proof-of-concept due to insufficient analytical validation [33], especially regarding precision and measurement variability. Accordingly, robust validation commonly includes the assessment of repeatability and intermediate precision supported by ANOVA-based designs [33-36], which helps determine whether variability originates from the device, the operator, or random measurement effects.

This study aims to validate an electrode fabricated using a 3D-printed acrylonitrile butadiene styrene (ABS) base, with the working and auxiliary electrodes filled with a carbon paste containing graphite, and the reference electrode and connectors filled with silver ink. Electrochemical validation was performed using the Randles-Ševčík equation, followed by statistical designs to identify validation through descriptive analyses and analysis of variance (ANOVA).

Experimental

Materials

Graphite powder and silver paint were purchased from Sigma Aldrich®. Potassium chloride was purchased from Synth®. Chloroform *p.a.* was purchased from Qhemis®. Potassium hexacyanoferrate was purchased from Carlo Erba®. 100 % mineral oil was purchased from União Química®. Transparent enamel from Colorama® and acrylonitrile butadiene styrene (ABS) filament were also used.

Instruments

The equipment used in this research included a 3D printer (GTMax, model A1, 0.45 mm extruder nozzle), two flat-angled bristle brushes (Bee Unique, 4 mm and 6 mm), and a portable potentiostat (PG581, Uniscan).

Development of the carbon paste modified printed electrode

The electrode design was created using Autodesk Inventor and fabricated with a 3D printer at 190 °C using ABS filament (Figure 1a). To prepare the carbon paste, 22.5 g of graphite powder was mixed with 7.5 g of mineral oil and homogenized by magnetic stirring in 100 mL of chloroform. The solvent was evaporated under stirring at room temperature (~23 °C) for approximately 10 minutes to achieve the desired consistency. The resulting paste was applied to the working and auxiliary electrodes using a brush (Figure 1b), while the reference electrode and all electrical connectors were filled with silver ink (Figure 1b). Finally, a hydrophobic barrier was created by coating the lower part of the electrodes with a layer of transparent enamel (Figure 1b).

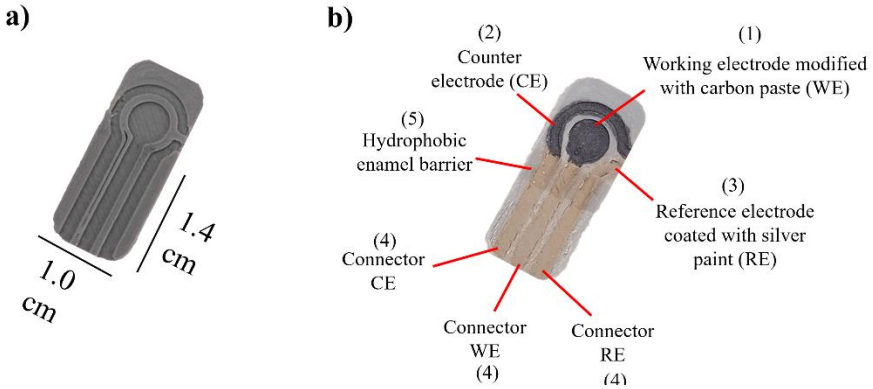

Figure 1. *(a) Base of the electrode printed in ABS, (b) base of the printed electrode filled with carbon paste on the working (1) and counter (2) electrodes, with silver ink on the pseudo-reference electrode (3), and their respective connectors (4) and a hydrophobic barrier coated with transparent enamel (5)*

Electrochemical validation

The electrodes were evaluated using cyclic voltammetry in a solution of potassium hexacyanoferrate (5 mmol L^{-1} $K_3[Fe(CN)_6]$) in 0.5 mol L^{-1} KCl. Measurements were performed over a potential range of -1.0 to 1.2 V (*vs*. Ag) at scan rates ranging from 10 to 250 mV s^{-1}. A UiEChem software, version 3.44 (Uniscan Instruments Ltd., UK) was used for these and all other voltammetric measurements with the potentiostat.

The electrochemical parameters related to the potential difference between oxidation and reduction peaks, $\Delta E_p = (E_{ap} - E_{cp})$, and the ratio of oxidation to reduction peak currents, i_{ap}/i_{cp}, were analysed. In addition, the electroactive area was determined using the appropriate form of the Randles-Ševčík equation, which, for a reversible system, is described by Equation (1):

$$i_p = 2.69\times10^5 A D_{1/2} n^{3/2} v^{1/2} C \quad (1)$$

where i_p / A is the peak current, A / cm² is the electroactive area, D / cm² s^{-1} is the diffusion coefficient, n is the number of electrons involved in the reaction, v / V s^{-1} is the potential scan rate and C / mol cm^{-3} is the concentration.

Statistical analysis

Statistical analyses were performed using data obtained from cyclic voltammetry. Ten electrodes were analysed, each performing five cycles in a solution of potassium hexacyanoferrate (5 mmol L^{-1} $K_3[Fe(CN)_6]$) in 0.5 mol L^{-1} KCl. Cyclic scans were conducted over a potential range of -1.0 to 1.2 V *vs*. Ag at a scan rate of 100 mV s^{-1}. Two parameters were evaluated: ΔE_p and the ratio i_{ap}/i_{cp}, extracted manually using Origin software (https://www.originlab.com) . Statistical analyses were carried out using Excel (from Microsoft, https://excel.cloud.microsoft) and RStudio (from Posit PBC, https://posit.co), with data normality verified by the Shapiro-Wilk test [37] and descriptive statistics performed prior to ANOVA. A second analyst (Analyst B), with no prior experience, repeated the analyses on a second set of 10 electrodes to assess reproducibility.

In this study, Analyst A has performed all steps related to electrode fabrication (ABS mold design and printing, carbon paste preparation, and electrode filling) as well as the preparation of the potassium hexacyanoferrate solution, following a standardized procedure. Analyst B was solely responsible for performing electrochemical measurements and statistical analysis using the prepared electrodes and solutions. This approach reflects a practical field application, where the end user receives ready-to-use electrodes and is responsible only for measurement and data interpretation. Therefore, reproducibility was specifically evaluated at the measurement stage. Descriptive analyses and one- and two-factor analyse of variance were conducted on the data from 100 voltammograms (50 from each analyst).

Descriptive analysis

Descriptive analysis summarizes key dataset characteristics, aiding in the identification of patterns and outliers [38]. Data from Analyst A was analysed for the two studied parameters (ΔE_p and i_{ap}/i_{cp}), then combined with Analyst B's data for comparative analysis. The main parameters obtained included the mean, standard error, median, mode, standard deviation, sample variance, skewness, kurtosis, and minimum and maximum values. Definitions of some of these parameters are provided below.

Skewness

A distribution is considered skewed when it is asymmetric around its central value. Skewness indicates how data are dispersed relative to the mean, median, and mode [39,40]. When the mean, median, and mode are equal, the distribution is symmetric (skewness ≈ 0). If mean > median and mode, the distribution has a longer right tail (positive skewness); if mean < median and mode, the left tail is longer (negative skewness).

Kurtosis

Kurtosis is a statistical measure that describes the "peakedness" of a distribution and provides insight into the behaviour of its tails [39,40]. A mesokurtic distribution resembles a normal curve, a leptokurtic distribution has a sharper peak with heavier tails (more extreme values), and a platykurtic distribution is flatter with lighter tails (fewer extreme values).

Standard error and standard deviation

Standard error and standard deviation are statistical measures of data variability. The standard error quantifies the accuracy of the sample mean as an estimate of the population mean, indicating how far the sample mean may deviate from the true mean [39-41]. The standard deviation measures the dispersion of individual data points around the dataset mean, reflecting overall variability [39-41].

Pearson's correlation

Within descriptive analysis, Pearson's correlation measures the strength and direction of the linear relationship between two continuous variables [39]. Values range from -1 (perfect negative correlation) to 1 (perfect positive correlation), with 0 indicating no linear correlation.

One-way analysis of variance

A one-way analysis of variance (ANOVA) was performed on cyclic voltammetry data of potassium hexacyanoferrate, as previously described. One-way ANOVA tests whether three or more population means are equal by analysing sample variances using a single factor [41]. The null hypothesis (H_0: $\mu_1 = \mu_2 = \mu_3$ …) is not rejected if the *p*-value > 0.05 or the F-value is below the critical *F*-value; otherwise, the alternative hypothesis (H_1: at least one mean differs) is accepted [40,41]. The analysis also provides the mean square (MS) within groups, used to calculate the coefficient of variation (CV, Equation (2)), which quantifies data dispersion, where $\bar{x}$ corresponds to the mean of the measured values. CV ≤ 15% indicates low dispersion, 15 to 30 % moderate, and ≥30 % high dispersion [40,41].

$$\mathrm{CV} = \frac{\sqrt{MS}}{\bar{x}} \quad (2)$$

Two-way analysis of variance

Reproducibility was assessed by evaluating the variation in parameter measurements performed by two analysts. Analyst B, an engineer without prior experience with the system, received instructions on equipment operation, analysis methodology, software handling, and parameter calculation. Two p-values were obtained for the fixed factors (analyst and electrode), using the same hypotheses as in the one-way ANOVA.

Results and discussion

Electrochemical validation

The fabricated electrodes were evaluated using a potassium hexacyanoferrate solution, a system widely reported in the literature for its well-established electrochemical behaviour. This redox couple typically exhibits two distinct voltammetric peaks, one for oxidation and one for reduction, corresponding to a reversible reaction, as described in Equation (3).

$$Fe(CN)_6^{3-} + e^- \leftrightarrow Fe(CN)_6^{4-} \quad (3)$$

Cyclic voltammograms obtained at a scan rate of 100 mV s^{-1} using the CP-SPE showed a peak current ratio (i_{ap}/i_{cp}) of 0.97, which is very close to the theoretical value of 1 expected for reversible systems, thereby indicating that the developed electrode is capable of reproducing the expected redox response of this probe [12].

Analysis of the potential difference between the oxidation and reduction peaks (ΔE_p) in the same voltammogram revealed a value of approximately 949 mV. The ΔE_p value expected for a reversible system is close to 59/*n* mV [12], where *n* is the number of electrons involved in the reaction, which in

this case is equal to 1. The discrepancy observed between the experimental and theoretical values can be ascribed to the quasi-reversible and irreversible electrochemical behaviour of the iron/ferricyanide system, particularly when non-conventional electrode materials, such as screen-printed or 3D-printed electrodes, are employed [42]. Such behaviour is strongly influenced by intrinsic properties of the electrode, including the chemical composition of the ink used during fabrication, the relative content of organic binders, the curing temperature, the presence of oxygenated surface species, the degree of surface hydrophilicity, and the specific nature of the electrode material [43,44].

Indeed, enlarged ΔE_p values have been widely reported for carbon pastes and screen-printed carbon electrodes compared to polished glassy carbon or metallic electrodes. Fanjul-Bolado *et al*. [44] demonstrated that screen-printed carbon electrodes often display significantly higher peak separations due to increased charge-transfer resistance and the presence of insulating binders within the carbon matrix, while Trachioti *et al*. [42] highlighted that graphite-based screen-printed platforms frequently deviate from ideal reversible behaviour because of surface heterogeneity and kinetic limitations. In contrast, electrodes fabricated by alternative deposition techniques, such as electro-deposition, sputtering, or mechanical polishing of glassy carbon, typically exhibit smaller ΔE_p values closer to the theoretical 59 mV expected for a one-electron reversible process [12], owing to the more compact and homogeneous nature of these surfaces, which favours faster heterogeneous electron-transfer kinetics. Therefore, the large ΔE_p observed for the present CP-SPE is consistent with the intrinsic characteristics of composite carbon paste-based and printed electrode architectures rather than an anomalous electrochemical response.

The investigation of scan rate variation in the $K_3[Fe(CN)_6]$ solution demonstrated a linear correlation between the anodic peak current (i_{ap}) and the square root of the scan rate ($v^{1/2}$), in agreement with the Randles-Ševčík equation, Equation (1). The voltammograms obtained at different scan rates are shown in Figure 2. These results enabled the determination of the electroactive surface area of the developed electrode.

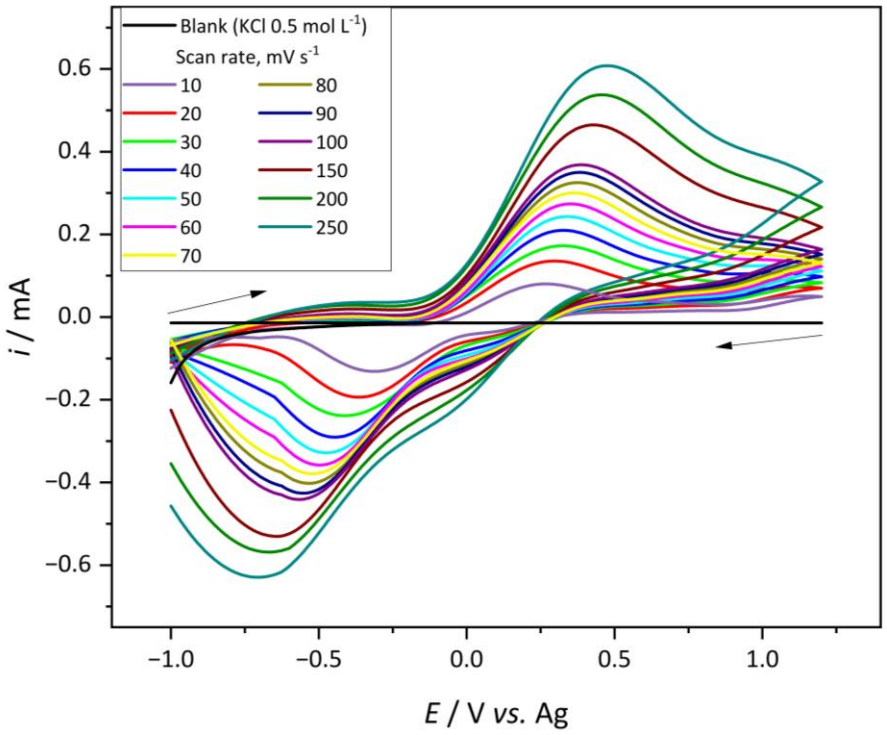

Figure 2. *Cyclic voltammograms for the analysis of 5.0 mmol L^{-1} $K_3[Fe(CN)_6]$ in 0.5 mol L^{-1} KCl using CP-SPE, at different scan rates*

For the calculation of the electroactive area, the Randles-Ševčík equation must be adapted, as its standard form Equation (1) applies only to reversible processes. For systems with $n\Delta E_p$ between 63 and 200 mV, the quasi-reversible form is used in Equation (4), while for $n\Delta E_p$>200 mV, the irreversible form is appropriate in Equation (5) [42].

$$i_p = \left(2.69\times10^5 AD^{1/2}n^{3/2}v^{1/2}C\right)K\left(\Lambda,\alpha\right) \quad (4)$$

$$i_p = 2.99\times10^5 AD^{1/2}v^{1/2}C\alpha^{1/2} \quad (5)$$

where $K(\Lambda,\alpha)$ is a dimensionless parameter for quasi-reversible reactions, and α is the charge transfer coefficient, reflecting the energy barrier symmetry for a single-electron step. The $n\Delta E_p$ values obtained from the voltammograms in Figure 2 exceeded 200 mV for all scan rates, indicating that Equation (5) is appropriate. α was calculated from the difference between the anodic peak potential (E_p) and the half-wave potential ($E_{p/2}$):

$$E_{p/2} = \frac{1.857RT}{\alpha F} = \frac{47.7}{\alpha} \ \left(\text{at } 25\,^{\circ}\text{C}\right) \quad (6)$$

where R is the universal gas constant (8.314 J mol^{-1} K^{-1}), T is the temperature in Kelvin, and F is the Faraday constant (96485 C mol^{-1}).

Using α in Equation (5), a linear relationship between the corrected peak current (i_{ap}) and the square root of scan rate ($v^{1/2}$) (Figure 3) was observed, yielding an electroactive area of 0.485 cm², 683 % larger than the geometric area (0.071 cm²). This enhancement is consistent with previous reports on carbon-based electrodes, in which surface roughness and porosity increase the number of accessible electrochemical sites. In the present system, the carbon paste with binder likely enhances surface heterogeneity and inner-sphere interactions of the $[Fe(CN)_6]^{3-/4-}$ redox couple, contributing to the increased effective area [45].

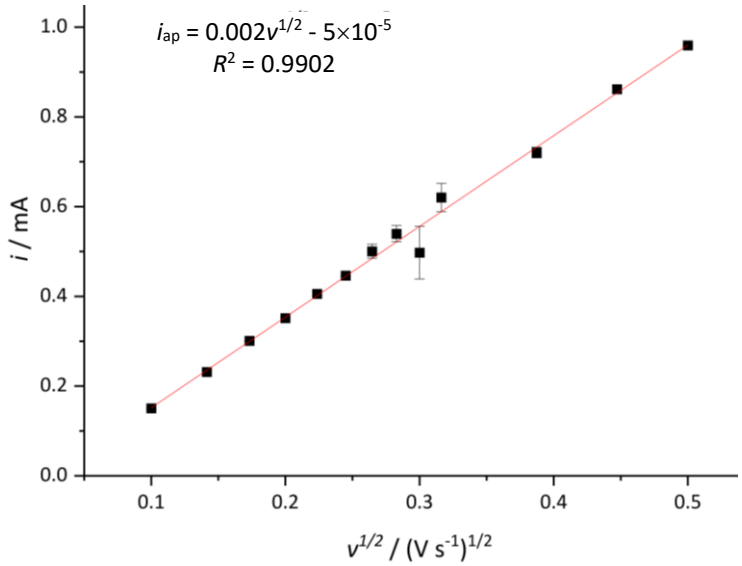

Figure 3. *Plot of the linear relationship between the anodic peak current (i_{ap}) corrected by the charge transfer coefficient (α), and the square root of the scan rate ($v^{1/2}$)*

Statistical analysis

Descriptive analysis

In Table 1, the main parameters obtained from the descriptive analysis of the data related to the two studied parameters (ΔE_p and i_{ap}/i_{cp}) with the analysis by Analyst A are presented.

For the ΔE_p parameter, the mean, median and mode were 0.721, 0.720, and 0.720, respectively, indicating a symmetrical distribution, consistent with the skewness value close to zero (0.439). This

suggests a cantered distribution with low variability. The kurtosis value (0.925) indicates a slightly leptokurtic distribution. Standard error and standard deviation were very low (0.002 and 0.012, corresponding to 0.3 and 1.7 % of the mean), and the variance was nearly zero, confirming minimal variation.

Table 1. *Main parameters obtained from the descriptive analysis of the data related to the two studied parameters (ΔE_p and i_{ap}/i_{cp}) with the analysis by Analyst A*

	ΔE_p / V	i_{ap}/i_{cp}
Mean	0.721	1.043
Standard error	0.002	0.007
Median	0.720	1.038
Mode	0.720	-
Standard deviation	0.012	0.051
Sample variance	0.000	0.003
Kurtosis	0.925	0.150
Skewness	0.439	0.455
Minimum	0.700	0.949
Maximum	0.755	1.184

For the i_{ap}/i_{cp} parameter, the absence of a mode precluded direct comparison with mean and median; however, the skewness (0.455) again indicated symmetry around the mean and low variability. The kurtosis value (0.150) was close to zero, consistent with a mesokurtic distribution. The standard error, standard deviation, and variance were 0.007, 0.051 and 0.003, corresponding to 0.7, 5.0 and 0.3 % of the mean, respectively, indicating low dispersion.

The data obtained from Analysts A and B were pooled and subjected to descriptive analysis, with results summarized in Table 2. Comparison with the data from Analyst A alone (Table 1) showed no significant changes in mean, median, or mode values. Kurtosis and skewness increased slightly but remained consistent with a symmetrical distribution for both parameters, with ΔE_p remaining slightly leptokurtic and i_{ap}/i_{cp} shifting from mesokurtic to slightly leptokurtic. Standard errors and standard deviations were low relative to the means, with values of 0.001 and 0.011 for ΔE_p, and 0.005 and 0.045 for i_{ap}/i_{cp}, corresponding to 0.1 and 1.5 % for ΔE_p, and 0.5 and 4.3 % for i_{ap}/i_{cp}, respectively. These findings confirm that the combined dataset preserves the distributional characteristics observed with Analyst A alone, demonstrating consistency between analysts and supporting good system reproducibility.

Table 2. *Main parameters obtained from the descriptive analysis of the data related to the two studied parameters (ΔE_p and i_{ap}/i_{cp}) from the Analyst A and Analyst B*

	ΔE_p / V	i_{ap}/i_{cp}
Mean	0.721	1.044
Standard error	0.001	0.005
Median	0.720	1.039
Mode	0.720	1.039
Standard deviation	0.011	0.045
Sample variance	1.663	0.766
Kurtosis	0.665	0.587
Skewness	0.700	0.949
Minimum	0.755	1.184

To evaluate the consistency of the two parameters (ΔE_p and i_{ap}/i_{cp}) across five measurements obtained from ten electrodes by Analyst A, as well as the agreement between data from Analysts A and B, Pearson's correlation was applied through pairwise comparisons. The results, presented in Figures 4a and 4b, show strong correlations in all cases, confirming high similarity within Analyst A's data and between the two analysts.

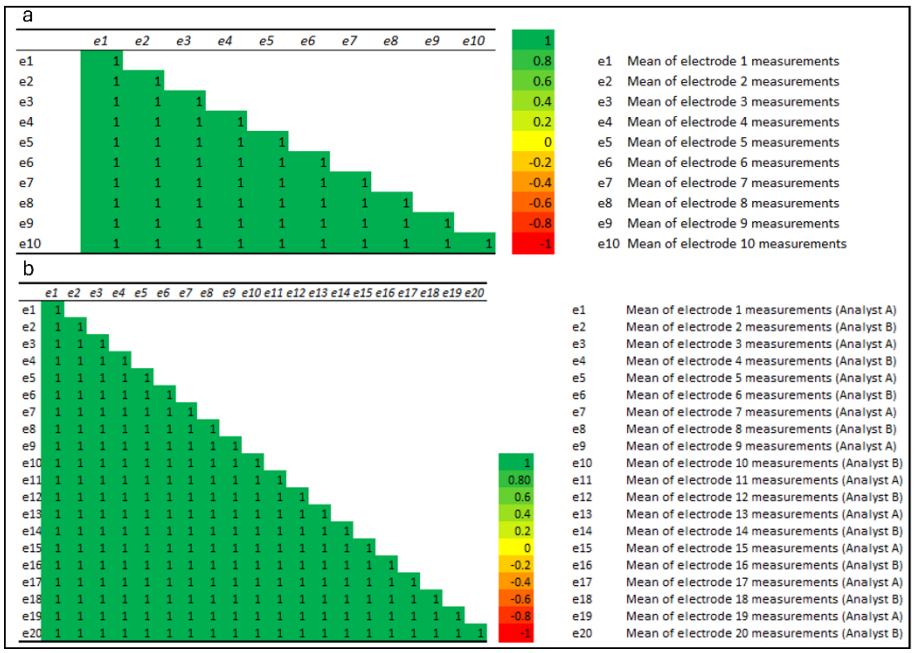

Figure 4. *Pearson correlation matrices of the mean values obtained from 5 measurements of two parameters (ΔE_p and i_{ap}/i_{cp}) for 10 electrodes. In both the x- and y-axes, e1 to e10 in (a) and e1 to e20 in (b) correspond to the mean measurements of each electrode, as specified on the right side of the figure. Each matrix cell represents the Pearson correlation coefficient between two electrodes. The matrices show (a) the results for Analyst A and (b) the combined results for Analyst A and Analyst B*

One-way analysis of variance

After assessing normality with the Shapiro-Wilk test (α = 0.05), the ΔE_p dataset yielded a *W* statistic, *i.e.* the Shapiro-Wilk test statistic, of 0.951, close to 1, indicating strong agreement with a normal distribution; the corresponding *p*-value was 0.386 (>0.05), and the null hypothesis of normality was therefore not rejected. Likewise, for the i_{ap}/i_{cp} dataset, *W* was 0.979 (also close to 1) and the *p*-value was 0.392 (>0.05), again indicating no evidence of departure from normality. Based on these results, one-way ANOVA was performed using the data obtained from Analyst A. Table 3 summarizes the mean square within groups (MS), *F*-values and *p*-values for each parameter (ΔE_p and i_{ap}/i_{cp}).

Table 3. *Values obtained for each parameter (ΔE_p and i_{ap}/i_{cp}) from the one-way ANOVA*

ΔE_p			i_{ap}/i_{cp}		
MS	*F*	Valor-*p*	MS	*F*	Valor-*p*
0.000	0.614	0.778	0.003	1.145	0.355

The *p*-values obtained from the ANOVA were 0.778 for ΔE_p and 0.355 for i_{ap}/i_{cp}, both higher than 0.05, indicating that the null hypothesis of equal means cannot be rejected. Similarly, the F-values for both parameters were lower than the critical *F*-value (2.124), indicating no significant differences among the electrode groups.

For the ΔE_p parameter, the MS value is 0, which corresponds to a CV (Equation 2) of 0, indicating low dispersion. For the i_{ap}/i_{cp} parameter, the MS value is 0.003, resulting in a CV of 5.25 %, indicating low dispersion. Serrano *et al*. [46] reported values ranging from 2.2 to 11.0 % for carbon screen-printed electrodes modified with multi-walled carbon nanotubes, carbon nanofibers, and graphene. The results obtained in the present study (0 and 5.25 %) fall within this reported range. Additionally, they are comparable to those described by Lotfi *et al.* [47], who found values of 3.6 and 4.5 % for a sensor based on Pd nanoparticles decorated poly-methyldopa (PMDA) modified TiO_2 nanoparticles on a glassy carbon electrode.

The similarity between the group means is also evident in the interval plots (Figure 5a and 5b), where the variance intervals of the means for all electrodes overlap for both parameters, indicating that all mean values are statistically equal.

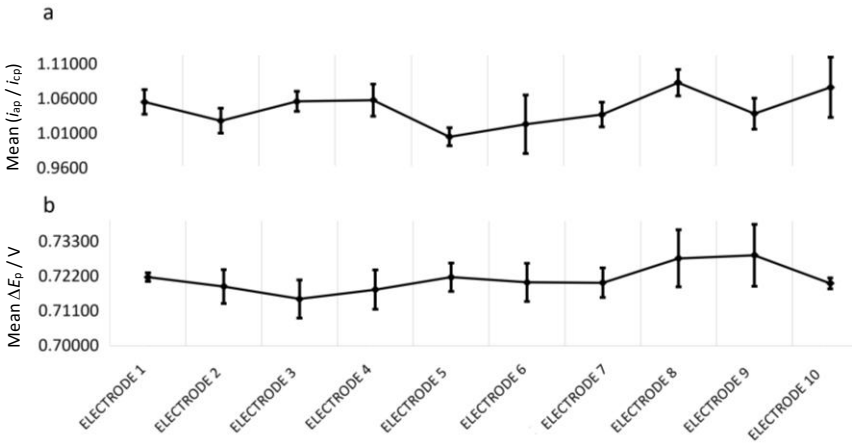

Figure 5. *Interval graph for (a)* i_{ap}/i_{cp} *and (b)* ΔE_p *averages for the 10 electrodes with a 95 % confidence interval*

Two-way analysis of variance

A two-factor ANOVA was performed using the results from both Analyst A and Analyst B. For the ΔE_p parameter, the *p*-values were 0.318 (electrode) and 0.528 (analyst), while for the i_{ap}/i_{cp} parameter, the values were 0.109 (electrode) and 0.865 (analyst). All p-values exceeded 0.05, indicating that the null hypothesis could not be rejected. Thus, neither the electrodes nor the analysts significantly contributed to measurement variability, and the results were statistically consistent across all 100 measurements.

Table 4 presents the results of the R&R (repeatability and reproducibility) and part-to-part studies, which evaluate the variability among the electrodes themselves, for both parameters. These analyses quantify the proportion of total variability attributable to the measurement system (R&R) versus the electrodes themselves. In this context, repeatability reflects the variation in measurements by the same analyst, whereas reproducibility captures variation between different analysts [40].

Table 4. *Study of variability for each parameter (*ΔE_p *and* i_{ap}/i_{cp}*) with the two-way ANOVA*

	Source	SD	Variance contribution, %
ΔE_p	Total measurement (R&R)	0.0114	100.00
	Repeatability	0.0114	100.00
	Reproducibility	0.0000	0.00
	Part-to-Part	0.0000	0.00
i_{ap}/i_{cp}	Total measurement (R&R)	0.0436	90.78
	Repeatability	0.0436	90.78

Reproducibility	0.0000	0.00
Part-to-Part	0.0139	9.22

For the ΔE_p parameter, 100 % of the variation originated from the R&R source, with no contribution from the part-to-part source. This indicates that the electrodes do not differ among themselves, and the minimal variability observed is due solely to the measurement system. Within the R&R source, all variation was attributed to repeatability, with no significant differences between analysts, demonstrating that the system is reproducible.

It is important to note that the comparison of measurements taken by two different analysts was intended to demonstrate the consistency of the results obtained with the developed electrodes. Even when the measurements and data analysis were performed by an operator with no prior experience in the technique, the results were comparable to those obtained by an experienced analyst. This result reinforces the robustness and simplicity of the method, showing that it can be reliably applied in the field by different users.

For the i_{ap}/i_{cp} parameter, there was a greater contribution of system variation attributed to the R&R source; however, 9.22 % of the total system variation was attributed to the part-to-part parameter, indicating that less than 10 % of the system's variation is due to differences between the parts (electrodes). Within the variation attributed to the R&R parameter, the entire contribution (90.78 %) comes from repeatability, once again showing that the system is reproducible.

Conclusions

The electrode developed from a 3D-printed ABS base, with working and auxiliary electrodes filled with carbon paste and a reference electrode filled with silver ink, was successfully evaluated both electrochemically and statistically. Electrochemical analysis using the Randles-Ševčík equation indicated irreversible behaviour with an electroactive area larger than the geometric area, likely due to the binder in the paste and inner-sphere reactions of the $Fe(CN)_6^{3-/4-}$ redox pair. Descriptive analyses showed data well-distributed around the mean, with low variability. One- and two-factor ANOVA confirmed good repeatability and reproducibility. Overall, the developed electrode was properly validated and demonstrates promising performance for voltammetric analyses.

Acknowledgements: *The authors are thankful to Teias Entrepreneurship and Innovation at Faculdade de Economia, Administração e Contabilidade de Ribeirão Preto, Universidade de São Paulo (FEARP-USP) for the 3D printing of the electrode bases.*

Funding: *This work was supported by CAPES - Finance Code 001, CAPES PROCAD/SPCF Process No. 88887.613955/2021-00, FAPESP - Process No. 2025/04394-0, CNPq - Process No. 302742/2022-0, and Instituto Nacional de Ciências e Tecnologia sobre Substâncias Psicoativas (INCTSP/CNPq) - grant number 406958/2022-0.*

References

[1] A. J. Saleh Ahammad, J. J. Lee, M. A. Rahman, Electrochemical sensors based on carbon nanotubes, *Sensors* **9** (2009) 2289-2319. https://doi.org/10.3390/s90402289

[2] N. R. Stradiotto, H. Yamanaka, M. Valnice, B. Zanoni, Electrochemical Sensors: A Powerful Tool in Analytical Chemistry, *Journal of the Brazilian Chemical Society* **14** (2003) 159-173. https://doi.org/10.1590/S0103-50532003000200003

[3] M. N. T. Silva, D . A. C. Alves, E. M. Richter, R. A. A. Munoz, E. Nossol, A simple, fast, portable and selective system using carbon nanotubes films and a 3D-printed device for monitoring hydroxychloroquine in environmental samples, *Talanta* **265** (2023) 124810. https://doi.org/10.1016/j.talanta.2023.124810

[4] R. A. A. Muñoz, Sustainable and economical platforms for electrochemical (bio)chemical sensing based on micro- and nanotechnologies, *Microchimica Acta* **190** (2023) 486. https://doi.org/10.1007/s00604-023-06058-6

[5] T. A. Matias, D. L. O. Ramos, L. V. Faria, A. de Siervo, E. M. Richter, R. A. A. Muñoz, 3D-printed electrochemical cells with laser engraving: developing portable electroanalytical devices for forensic applications, *Microchimica Acta* **190** (2023) 297. https://doi.org/10.1007/s00604-023-05872-2

[6] C. D. Lima, L. M. de A. Melo, L. C. Arantes, N. dos S. Conceição, I. de F. Schaffel, L. L. Machado, R. de Q. Ferreira, W. T. P. dos Santos, Simple and selective screening method for the synthetic cathinone MDPT in forensic samples using carbon nanofiber screen-printed electrodes, *Talanta* **269** (2024) 125375. https://doi.org/10.1016/j.talanta.2023.125375

[7] A. dos S. Novais, D. G. Ribeiro, L. M. de A. Melo, E. F. Júnior, L. C. Arantes, B. G. Lucca, E. I. de Melo, R. F. Brocenschi, W. T. P. dos Santos, R. A. B. da Silva, Simple, Miniaturized, Adaptable, Robust and Transportable (SMART) 3D-printed electrochemical cell: A friendly tool for on-site and forensic analysis, *Sensors & Actuators B* **398** (2024) 134667. https://doi.org/10.1016/j.snb.2023.134667

[8] A. A. Macedo, L. C. Arantes, D. M. Pimentel, T. de D. Melo, L. M. de A. Melo, W. A. de Barros, C. M. Rocha, Â. de Fátima, W. T. P. dos Santos, Comprehensive detection of lysergic acid diethylamide (LSD) in forensic samples using carbon nanotube screen-printed electrodes, *Analytical Methods* **15** (2023) 5837-5845. https://doi.org/10.1039/d3ay01385e

[9] R. M. Cardoso, D. M. H. Mendonça, W. P. Silva, M. N. T. Silva, E. Nossol, R. A. B. da Silva, E. M. Richter, R. A. A. Muñoz, 3D printing for electroanalysis: From multiuse electrochemical cells to sensors, *Analytica Chimica Acta* **1033** (2018) 49-57. https://doi.org/10.1016/j.aca.2018.06.021

[10] H. Karimi-Maleh, F. Karimi, M. Alizadeh, A. L. Sanati, Electrochemical Sensors, a Bright Future in the Fabrication of Portable Kits in Analytical Systems, *Chemical Record* **20** (2020) 682-692. https://doi.org/10.1002/tcr.201900092

[11] N. R. Stradiotto, H. Yamanaka, M. V. B. Zanoni, M. D. P. T. Sotomayor, *Métodos eletroanalíticos: conceitos, experimentos e aplicações*, Cultura Acadêmica, São Paulo, 2021, p. 13-24, 133-142. ISBN: 978-6559541751. (In Portuguese)

[12] A. J. Bard, L. R. Faulkner, *Electrochemical methods: fundamentals and applications*, 2ª, John Wiley & Sons, INC., New York, 2001, p. 1-6, 503 ISBN: 978-0471043720.

[13] O. D. Renedo, M. A. Alonso-Lomillo, M. J. A. Martínez, Recent developments in the field of screen-printed electrodes and their related applications, *Talanta* **73** (2007) 202-219. https://doi.org/10.1016/j.talanta.2007.03.050

[14] R. D. Crapnell, A. G. M. Ferrari, N. C. Dempsey, C. E. Banks, Electroanalytical overview: screen-printed electrochemical sensing platforms for the detection of vital cardiac, cancer and inflammatory biomarkers, *Sensors and Diagnostics* **1** (2022) 405-428. https://doi.org/10.1039/d1sd00041a

[15] P. M. Kalligosfyri, A. Miglione, S. Cinti, Screen-Printing and 3D-Printing Technologies in Electrochemical (Bio)sensors: Opportunities, Advantages and Limitations, *ECS Sensors Plus* **4** (2025) 010601. https://doi.org/10.1149/2754-2726/ada395

[16] M. Pohanka, Screen Printed Electrodes in Biosensors and Bioassays. A Review, *International Journal of Electrochemical Science* **15** (2020) 11024-11035. https://doi.org/10.20964/2020.11.19

[17] S. Park, S. Ban, N. Zavanelli, A. E. Bunn, S. Kwon, H. R. Lim, W. H. Yeo, J. H. Kim, Fully Screen-Printed PI/PEG Blends Enabled Patternable Electrodes for Scalable Manufacturing of Skin-Conformal, Stretchable, Wearable Electronics, *ACS Applied Materials and Interfaces* **15** (2023) 2092-2103. https://doi.org/10.1021/acsami.2c17653

[18] Z. Yhobu, M. Sreeramareddygari, C. Phanthong, S. Budagumpi, D. H. Nagaraju, W. Chaiworn, M. Somasundrum, P. Rijiravanich, S. Chuangchote, W. Surareungchai, Gel-derived NiO-MoS_2 for the scalable fabrication of bifunctional screen-printed electrodes for overall water splitting, *International Journal of Hydrogen Energy* **139** (2025) 247-256. https://doi.org/10.1016/j.ijhydene.2025.05.296

[19] E. M. Materon, A. Wong, L. M. Gomes, G. Ibáñez-Redín, N. Joshi, O. N. Oliveira, R. C. Faria, Combining 3D printing and screen-printing in miniaturized, disposable sensors with carbon paste electrodes, *Journal of Materials Chemistry C* **9** (2021) 5633-5642. https://doi.org/10.1039/d1tc01557e

[20] Z. Taleat, A. Khoshroo, M. Mazloum-Ardakani, Screen-printed electrodes for biosensing: A review (2008-2013), *Microchimica Acta* **181** (2014) 865-891. https://doi.org/10.1007/s00604-014-1181-1

[21] V. A. O. P. Silva, W. S. Fernandes-Junior, D. P. Rocha, J. S. Stefano, R. A. A. Munoz, J. A. Bonacin, B. C. Janegitz, 3D-printed reduced graphene oxide/polylactic acid electrodes: A new prototyped platform for sensing and biosensing applications, *Biosensors & Bioelectronics* **170** (2020) 112684. https://doi.org/10.1016/j.bios.2020.112684

[22] M. Li, Y. T. Li, D. W. Li, Y. T. Long, Recent developments and applications of screen-printed electrodes in environmental assays-A review, *Analytica Chimica Acta* **734** (2012) 31-44. https://doi.org/10.1016/j.aca.2012.05.018

[23] C. Wanklyn, D. Burton, E. Enston, C. A. Bartlett, S. Taylor, A. Raniczkowska, M. Black, L. Murphy, Disposable screen printed sensor for the electrochemical detection of delta-9-tetrahydrocannabinol in undiluted saliva, *Chemistry Central Journal* **10** (2016) 1. https://doi.org/10.1186/s13065-016-0148-1

[24] É. N. Oiye, M. F. M. Ribeiro, B. Ferreira, R. C. B. Botelho, M. F. de Oliveira, Disposable 3D Printed Electrode for the Electrochemical Detection of Delta-9-Tetrahydrocannabinol in Aqueous Solution and 11-Nor-9-Carboxy-Tetrahydrocannabinol in Saliva, *Brazilian Journal of Forensic Sciences, Medical Law and Bioethics* **9** (2020) 521-533. https://doi.org/10.17063/bjfs9(4)y2020521-533

[25] M. A. Balbino, É. N. Oiye, M. F. M. Ribeiro, J. W. C. Júnior, I. C. Eleotério, A. J. Ipólito, M. F. de Oliveira, Use of screen-printed electrodes for quantification of cocaine and Δ^9-THC: adaptions to portable systems for forensic purposes, *Journal of Solid State Electrochemistry* **20** (2016) 2435-2443. https://doi.org/10.1007/s10008-016-3145-3

[26] T. Pholsiri, A. Lomae, K. Pungjunun, S. Vimolmangkang, W. Siangproh, O. Chailapakul, A chromatographic paper-based electrochemical device to determine Δ^9-tetrahydrocannabinol and cannabidiol in cannabis oil, *Sensors & Actuators, B: Chemical* **355** (2022) 131353. https://doi.org/10.1016/j.snb.2021.131353.

[27] A. G. M. Ferrari, S. J. Rowley-Neale, C. E. Banks, Screen-printed electrodes: Transitioning the laboratory in-to-the field, *Talanta Open* **3** (2021) 100032. https://doi.org/10.1016/j.talo.2021.100032

[28] R. R. Suresh, M. Lakshmanakumar, J. B. B. A. Jayalatha, K. S. Rajan, S. Sethuraman, U. M. Krishnan, J. B. B. Rayappan, Fabrication of screen-printed electrodes: opportunities and challenges, *Journal of Materials Science* **56** (2021) 8951-9006. https://doi.org/10.1007/s10853-020-05499-1

[29] G. Paimard, E. Ghasali, M. Baeza, Screen-Printed Electrodes: Fabrication, Modification, and Biosensing Applications, *Chemosensors* **11** (2023) 113. https://doi.org/10.3390/chemosensors11020113

[30] D. A. Skoog, D. West, J. Holler, S. Crouch, *Fundamentos de Química Analítica*, Cengage Learning, São Paulo, 2006, p. 183 ISBN: 978-8522104369. (In Portuguese)

[31] C. Zuidema, C. S. Schumacher, E. Austin, G. Carvlin, T. V. Larson, E. W. Spalt, M. Zusman, A. J. Gassett, E. Seto, J. D. Kaufman, L. Sheppard, Deployment, calibration, and cross-validation of low-cost electrochemical sensors for carbon monoxide, nitrogen oxides, and ozone for an epidemiological study, *Sensors* **21** (2021) 4214. https://doi.org/10.3390/s21124214
[32] E. Desimoni, B. Brunetti, Presenting Analytical Performances of Electrochemical Sensors. Some Suggestions, *Electroanalysis* **25** (2013) 1645-1651. https://doi.org/10.1002/elan.201300150
[33] J. V. F. Paiva, D. A. de Azevedo, P. V. V. Romanholo, S. A. S. Machado, M. L. Felsner, A. Galli, L. F. Sgobbi, Disposable electrochemical sensor modified with gold nanostructures for rapid and eco-friendly nitrite detection in tap water: From fabrication to robust analytical validation, *Microchemical Journal* **220** (2026) 116358. https://doi.org/10.1016/j.microc.2025.116358
[34] M. A. Abdel Rahman, S. A. Atty, S. S. El-Mosallamy, M. R. Elghobashy, H. E. Zaazaa, A. S. Saad, Experimentally designed electrochemical sensor for therapeutic drug monitoring of Ondansetron co-administered with chemotherapeutic drugs, *BMC Chemistry* **16** (2022) 77. https://doi.org/10.1186/s13065-022-00871-5
[35] L. L. Cabral, C. Kalinke, M. G. P. Valenga, L. H. Marcolino-Junior, M. F. Bergamini, Biochar for Electrochemical Sulfanilamide Detection: Comparative Evaluation of Carbon Paste and Screen-Printed Electrodes, *ACS Omega* **10** (2025) 33595-33606. https://doi.org/10.1021/acsomega.5c04276
[36] A. Badameh, A. Nezhadali, A disposable homemade screen printed electrode for famotidine analysis using a computer-designed molecularly imprinted polymer based on the MWCNT-Fe_3O_4 nanocomposite in simulated real samples, *Analytical Methods* **16** (2024) 7534-7545. https://doi.org/10.1039/d4ay01122h
[37] S. S. Shapiro, M. B. Wilk, An analysis of variance test for normality (complete samples), *Biometrika*, 52(3-4) (1965) 591-611. https://doi.org/10.1093/biomet/52.3-4.591
[38] R. Larson, B. Farber, *Estatística Aplicada*, Pearson, São Paulo, 2009, p. 31-32, 82. ISBN: 978-8576053729 (In Portuguese)
[38] D. C. Montgomery, G. C. Runger, *Estatística Aplicada e Probabilidade para Engenheiros*, LTC, Rio de Janeiro, 2024, p. 107-110, 119-122, 145. ISBN: 978-8521637332 (In Portuguese)
[39] L. P. Fávero, P. Belfiore, *Manual de Análise de Dados: Estatística e Modelagem Multivariada com Excel®, SPSS® e Stata®*, Elsevier, Rio de Janeiro, 2017, p. 63-66, 227-242. ISBN: 978-8535270877. (In Portuguese)
[40] M. F. Triola, *Essentials of Statistics*, Pearson, Boston, 2015, p. 97, 561-570. ISBN: 0-321-92459-2.
[41] M. G. Trachioti, A. C. Lazanas, M. I. Prodromidis, Shedding light on the calculation of electrode electroactive area and heterogeneous electron transfer rate constants at graphite screen-printed electrodes, *Microchimica Acta* **190** (2023) 251. https://doi.org/10.1007/s00604-023-05832-w
[42] C. E. Banks, T. J. Davies, G. G. Wildgoose, R. G. Compton, Electrocatalysis at graphite and carbon nanotube modified electrodes: Edge-plane sites and tube ends are the reactive sites, *Chemical Communications* (2005) 829-841. https://doi.org/10.1039/b413177k
[43] P. Fanjul-Bolado, D. Hernández-Santos, P. J. Lamas-Ardisana, A. Martín-Pernía, A. Costa-García, Electrochemical characterization of screen-printed and conventional carbon paste electrodes, *Electrochimica Acta* **53** (2008) 3635-3642. https://doi.org/10.1016/j.electacta.2007.12.044
[44] A. G. M. Ferrari, C. W. Foster, P. J. Kelly, D. A. C. Brownson, C. E. Banks, Determination of the electrochemical area of screen-printed electrochemical sensing platforms, *Biosensors* **8** (2018) 53. https://doi.org/10.3390/bios8020053
[45] N. Serrano, Ò. Castilla, C. Ariño, M. S. Diaz-Cruz, J. M. Díaz-Cruz, Commercial screen-printed electrodes based on carbon nanomaterials for a fast and cost-effective voltammetric

determination of paracetamol, ibuprofen and caffeine in water samples, *Sensors* **19** (2019) 4039. https://doi.org/10.3390/s19184039

[46] S. Lotfi, H. Veisi, B. Karmakar, A convenient strategy for the electrochemical evaluation of acetaminophen and caffeine in combined drugs and biological samples over TiO_2@polymethyldopa/Pd nanocomposite functionalized glassy carbon electrodes, *Measurement* **186** (2021) 110156. https://doi.org/10.1016/j.measurement.2021.110156